

# **RealSyn: An Effective and Scalable Multimodal Interleaved Document Transformation Paradigm**

Tiancheng Gu<sup>♥\*</sup>, Kaicheng Yang<sup>♣\*</sup>, Chaoyi Zhang<sup>♥</sup>, Yin Xie<sup>♣</sup>, Xiang An<sup>♣</sup>,  
Ziyong Feng<sup>♣</sup>, Dongnan Liu<sup>♥</sup>, Weidong Cai<sup>♥†</sup>, Jiankang Deng<sup>♣†</sup>

<sup>♥</sup>The University of Sydney <sup>♣</sup>DeepGlint <sup>♣</sup>Imperial College London  
tigu8498@uni.sydney.edu.au, kaichengyang@deepglint.com

 [Project Page](#)

 [Code](#)

## Abstract

After pre-training on extensive image-text pairs, Contrastive Language-Image Pre-training (CLIP) demonstrates promising performance on a wide variety of benchmarks. However, a substantial volume of multimodal interleaved documents remains underutilized for contrastive vision-language representation learning. To fully leverage these unpaired documents, we initially establish a Real-World Data Extraction pipeline to extract high-quality images and texts. Then we design a hierarchical retrieval method to efficiently associate each image with multiple semantically relevant realistic texts. To further enhance fine-grained visual information, we propose an image semantic augmented generation module for synthetic text production. Furthermore, we employ a semantic balance sampling strategy to improve dataset diversity, enabling better learning of long-tail concepts. Based on these innovations, we construct *RealSyn*, a dataset combining realistic and synthetic texts, available in three scales: 15M, 30M, and 100M. We compare our dataset with other widely used datasets of equivalent scale for CLIP training. Models pre-trained on *RealSyn* consistently achieve state-of-the-art performance across various downstream tasks, including linear probe, zero-shot transfer, zero-shot robustness, and zero-shot retrieval. Furthermore, extensive experiments confirm that *RealSyn* significantly enhances contrastive vision-language representation learning and demonstrates robust scalability.



## Keywords

large-scale image-text dataset, vision-language representation learning, multimodal interleaved document

## 1 Introduction

The rapid proliferation of mobile networks and social platforms has led to exponential growth in large-scale data, offering a robust foundation for contrastive vision-language representation learning [2, 25–27, 81, 84, 88]. By predicting the correspondence between images and description texts, Contrastive Language-Image Pre-training (CLIP) [62] pre-trains separate uni-modal encoders

*Example of interleaved image-text documents:*

.....  There are many different standards of analog video. Most are conceptually similar, but they have varying numbers of signal channels.  They are all based on the analog signal(s) drawing the.....



*How to utilize interleaved documents for CLIP training?  
How to leverage realistic&synthetic texts to enhance CLIP?*

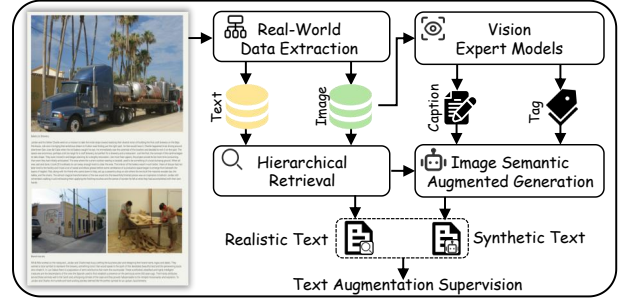


**Figure 1: Multimodal interleaved documents are unsuitable for CLIP training. We construct distinct image-text pairs from such documents via retrieval and generation.**

and achieves excellent performance across a range of downstream tasks, including image captioning [44, 56], object detection [49, 77], and semantic segmentation [29, 51, 87]. Notably, the representational capacity of such models improves significantly with the scale of the training dataset [48]. Designing a new data paradigm to expand the scale and diversity of image-text datasets, thereby continuously improving the capabilities of pre-trained vision-language representations, represents a significant and challenging issue.

In recent years, the introduction of large-scale image-text pair datasets [8, 21, 64, 65, 71] has substantially advanced vision-language representation learning. Due to download failures and non-English captions in the YFCC [71] dataset, DeCLIP [47] reprocesses a new version of the YFCC15M dataset. LAION400M [65] provides 400 million image-text pairs collected from the web and filtered using CLIP similarity. COYO700M [8] offers 747 million high-quality pairs curated through advanced filtering strategies, including CLIP similarity, watermark detection, and aesthetic scoring. Despite these advancements, a substantial amount of non-paired data, particularly interleaved image-text documents [43, 45, 89] containing multiple images and text paragraphs without explicit correspondence, remains incompatible with conventional vision-language representation learning methods.

\* Equal Contribution

† Corresponding Author.



This work is licensed under a Creative Commons Attribution 4.0 International License.  
MM '25, Dublin, Ireland

© 2025 Copyright held by the owner/author(s).

ACM ISBN 979-8-4007-2035-2/2025/10

<https://doi.org/10.1145/3746027.3755098>

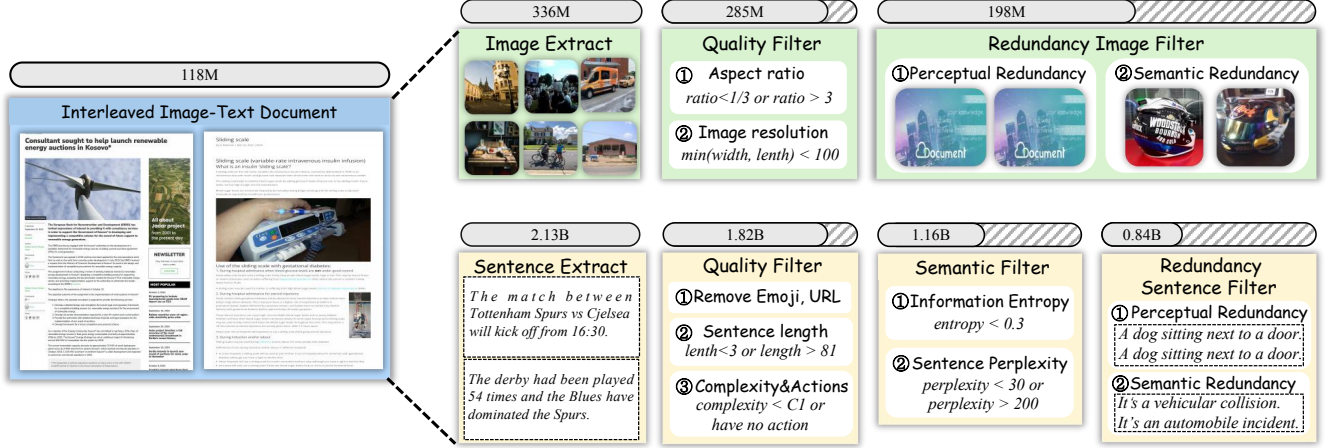


**Figure 2: The Real-World Data Extraction pipeline to extract high-quality images and texts from interleaved image-text documents.**

Recent studies [19, 42, 83, 85] aim to enhance the quality of open-source image-text datasets using existing models. For instance, LaCLIP [19] leverages large language models (LLMs) to rewrite raw captions for better alignment with images. CapsFusion [83] fine-tunes an LLM using a ChatGPT-generated instruction dataset to mitigate hallucination issues. DreamLIP [85] re-captions 30 million images with detailed descriptions using a pre-trained large multimodal model. However, these methods primarily enhance data quality by focusing on synthetic data, thereby overlooking the significance of real-world data. Moreover, the diversity and distribution of synthetic captions produced by these approaches are inherently restricted by the limitations of the underlying generative models.

In this paper, we explore two fundamental questions: 1) **How to utilize multimodal interleaved documents for CLIP training.** 2) **How to effectively leverage both realistic and synthetic texts to enhance CLIP performance.** As depicted in Figure 1, we initially develop a Real-World Data Extraction pipeline to extract high-quality images and texts from real-world multimodal interleaved documents. Subsequently, we design a hierarchical retrieval method to efficiently associate each image with multiple semantically relevant texts. To improve fine-grained image understanding, we introduce a visual semantic augmented generation module for synthetic text production. Additionally, we implement a semantic balance sampling strategy to enhance dataset diversity and facilitate the learning of long-tail concepts. Leveraging these innovations, we construct the *RealSyn* dataset, which incorporates both realistic and synthetic texts in three sizes: 15M, 30M, and 100M. We evaluate the *RealSyn* dataset against other widely used datasets of similar scale for CLIP training. Models pre-trained on *RealSyn* consistently demonstrate state-of-the-art performance on various downstream tasks, including linear probe, zero-shot transfer, zero-shot robustness, and zero-shot retrieval. Extensive experiments validate that *RealSyn* is effective for contrastive vision-language representation learning and shows excellent scalability. The main contributions of this paper are summarized as follows:

- We propose an **effective and scalable multimodal interleaved document transformation paradigm** for contrastive vision-language representation learning.
- We release *RealSyn*, a **large-scale semantic balanced dataset** that integrates both realistic and synthetic texts and is available in three sizes: 15M, 30M, and 100M.
- We conduct **extensive experiments** and demonstrate the effectiveness and scalability of our proposed *RealSyn* dataset for CLIP training.

## 2 Related Work

**Large-Scale Pre-training Dataset.** In recent years, several large-scale image-text datasets [8, 12, 15, 23, 46] collected from the Internet have been released. The YFCC100M [71] dataset provides a comprehensive overview of the evolution of photo and video documentation and sharing from the inception of Flickr in 2004 until early 2014. Due to download failures and non-English captions, DeCLIP [47] reprocesses a new version of the YFCC15M dataset. Additionally, the LAION400M [65] dataset contains 400 million image-text pairs collected from Common Crawl and widely used in vision-language pre-training. Recent advancements have also introduced several large-scale interleaved image-text document datasets [43, 45, 89]. The OBELICS [43] dataset uses a comprehensive filtering strategy and includes 141 million web pages, 353 million associated images, and 115 billion text tokens extracted from Common Crawl. However, due to data format constraints and training inefficiencies, interleaved image-text documents are currently unsuitable for CLIP training.

**Vision Language Pre-training.** As a pioneering work in visual language pre-training, CLIP has attracted extensive attention due to its powerful zero-shot recognition and exceptional transfer learning performance [24, 31, 55, 66, 69, 74]. Inspired by CLIP, numerous visual-language pre-training works have been published in recent years [47, 57, 79]. SLIP [57] enhances performance by combining

self-supervised learning with CLIP pre-training. DeCLIP [47] increases pre-training efficiency by integrating multi-view supervision across modalities and nearest-neighbor supervision from similar pairs. To mitigate the influence of noisy data, ALIP [79] introduces a gating mechanism that dynamically allocates weights to samples. Despite their advancements, these methods primarily depend on large-scale image-text pairs derived from the Internet. Recent studies [48, 76] demonstrate that the capabilities of CLIP enhance with the expansion of high-quality image-text datasets. Given the extensive use of internet-derived image-text data in existing datasets, there is a pressing need to develop a new data construction paradigm to further expand the scale of high-quality image-text data.

**Synthetic Captions.** Recent works [10, 79, 83] indicate that image-text pairs obtained from websites contain intrinsic noise, which directly impacts the effectiveness of vision-language pre-training. To enhance the quality of existing datasets, LaCLIP [19] uses the in-context learning capability of large language models to rewrite text descriptions associated with each image. CapsFusion [83] employs large language models to refine information from web-based image-text pairs and synthetic captions, improving the quality of multimodal pre-training data. Similarly, DreamLIP [85] generates detailed descriptions for 30 million images using a pretrained large multimodal model. Nevertheless, these methods predominantly focus on synthetic data enhancement, neglecting the importance of real-world data. Furthermore, the diversity and distribution of synthetic captions generated by these methods are intrinsically constrained by the capabilities of the generative models employed.

### 3 RealSyn Dataset

#### 3.1 Real-World Data Extraction

To transform interleaved image-text documents for vision-language representation learning, we establish a Real-World Data Extraction pipeline (Figure 2) to extract high-quality images and texts. This pipeline consists of three steps: Data Extraction, Image Filtration, and Sentence Filtration.

**Data Extraction.** We employ 118M interleaved image-text documents from the OBELICS [43] as the primary data source. All images are extracted and stored in a dedicated image database, while sentences are segmented using the Natural Language Toolkit (NLTK) [5] and stored in a separate sentence database. This process yields 336M images and 2.13B sentences from the interleaved documents.

**Image Filtration.** After extracting 336M images, we apply a two-stage filtering process to ensure data quality and reduce redundancy. First, we discard images that meet any of the following criteria: 1) the shorter dimension is fewer than 100 pixels, or 2) the aspect ratio exceeds 3 or is below 1/3. This step removes 51M low-quality images. Next, following CLIP-CID [80], we use the EVA02-CLIP E/14-plus model [68] to extract image embeddings and apply the Union-Find algorithm [70] to eliminate perceptually and semantically redundant images. This step removes an additional 87M images, resulting in a refined dataset of 198M high-quality images.

**Sentence Filtration.** After extracting 2.13B sentences from interleaved image-text documents, we conduct rigorous filtering based

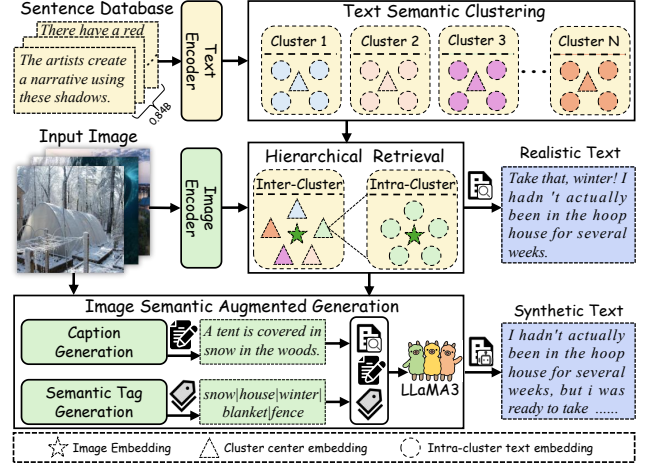


**Figure 3: The architecture of our proposed framework, which constructs distinct image-text pairs from real-world data extracted from interleaved documents via retrieval and generation.**

on quality, semantics, and redundancy. Initially, we eliminate sentences based on the following criteria: 1) presence of emojis or URLs; 2) sentences containing fewer than 3 or more than 81 words; and 3) following CAT [61], we retain samples with at least C1 caption complexity and incorporating an action. This phase reduces the corpus size from 2.13B to 1.82B sentences. Then we apply semantic filtering to the remaining sentences, eliminating those with minimal information assessed through information entropy:

$$\theta(x) = - \sum_{i=1}^n p(x_i) \log p(x_i), \quad (1)$$

where  $n$  denotes the number of words in a sentence,  $x_i$  represents the  $i$ -th words in the sentences  $x$ , and  $p(x_i)$  is the probability of the word  $x_i$  in the entire corpus. Based on human cognition principles and empirical experience, we filter out sentences with a score below 0.3. To further refine the corpus by removing difficult or ambiguous sentences, we use GTP2-large [63] to calculate the perplexity score  $\mathcal{PPL}$  for each sentence:

$$\mathcal{PPL}(x) = \exp \left\{ - \frac{1}{t} \sum_{i=1}^t \log p_{\theta}(x_i | x_{<i}) \right\}, \quad (2)$$

where  $t$  represents the token number of the sentence, and  $p_{\theta}(x_i | x_{<i})$  is the likelihood of the  $i$ -th token given the previous tokens. We engage three human experts to determine the minimum and maximum values of the perplexity interval for high-quality sentences by comparing sentences of varying perplexity levels. Sentences within the average minimum (30) and maximum perplexity (200) intervals are retained. The overall semantics filtering reduces the corpus to 1.16B sentences. In the final stage, similar to redundancy image filtering, we perform both perceptual and semantic deduplication of sentences. This process results in a refined corpus of 0.84B sentences that include extensive real-world knowledge.



**Table 1: Linear probe on 20 downstream datasets. Pre-training ViT-B/32 on *RealSyn* achieves 1.3%-6.9% average performance improvement.**

Data Scale	Dataset	Food101	CIFAR10	CIFAR100	Birdsnap	SUN397	Cars	Aircraft	DTD	Pets	Caltech	Flowers	STL10	EuroSAT	RESISC45	KITTI	Country	UCF101	Memes	SST2	ImageNet	Average
15M	YFCC	67.2	90.4	70.8	47.7	66.7	23.8	29.7	62.4	65.7	80.1	90.0	94.7	94.9	79.4	75.4	18.4	70.8	48.6	56.2	56.7	64.5
	LAION	71.0	93.3	78.1	41.0	66.3	76.9	43.0	71.2	74.5	87.6	88.2	93.6	95.3	82.9	72.2	13.5	75.4	55.7	57.3	59.3	69.8
	<i>RealSyn</i>	77.1	94.5	78.7	43.4	71.4	64.7	42.7	71.3	79.9	90.0	88.2	96.4	96.2	87.2	72.4	16.7	79.9	55.7	57.7	64.0	71.4
30M	LAION	76.1	94.5	80.0	47.4	70.3	82.3	45.9	74.7	80.3	89.8	89.5	95.6	95.5	84.5	72.6	15.2	76.6	56.2	60.0	64.3	72.6
	<i>RealSyn</i>	81.2	95.4	81.8	48.4	74.5	73.4	45.2	74.2	84.1	91.3	90.6	97.2	96.5	89.2	74.5	19.0	82.6	55.0	56.2	68.5	73.9
100M	LAION	80.2	95.7	82.5	51.3	73.4	85.3	46.1	75.6	83.2	91.1	92.0	96.9	95.2	85.9	68.4	17.4	80.0	57.3	61.4	68.3	74.4
	<i>RealSyn</i>	84.2	96.3	83.5	54.0	76.2	77.4	47.6	75.6	86.3	92.1	91.7	97.7	96.8	90.6	73.1	21.1	83.7	57.3	58.9	71.6	75.8

**Table 2: Zero-shot transfer on 20 downstream datasets. Pre-training ViT-B/32 on *RealSyn* achieves 2.3%-14.3% average performance improvement.**

Data Scale	Dataset	Food101	CIFAR10	CIFAR100	Birdsnap	SUN397	Cars	Aircraft	DTD	Pets	Caltech	Flowers	STL10	EuroSAT	RESISC45	KITTI	Country	UCF101	Memes	SST2	ImageNet	Average
15M	YFCC	36.3	74.0	40.3	19.4	41.8	2.1	2.3	12.0	19.8	59.8	48.9	87.7	21.2	20.3	23.8	5.1	27.8	47.4	50.1	32.3	33.6
	LAION	49.1	85.7	56.9	11.5	45.1	49.9	3.8	25.7	54.6	78.1	30.5	89.5	36.7	36.1	21.7	5.6	38.2	48.8	49.9	37.1	42.7
	<i>RealSyn</i>	60.0	85.7	58.3	10.5	56.4	27.6	5.5	33.2	61.7	80.2	31.2	92.4	56.5	56.2	34.0	8.9	52.6	53.3	51.3	43.3	47.9
30M	LAION	58.9	85.9	63.1	17.4	54.8	61.0	4.3	36.4	65.5	82.0	41.3	91.3	40.3	43.7	24.3	7.2	47.4	51.5	50.1	44.9	48.6
	<i>RealSyn</i>	67.5	89.0	65.2	15.0	60.6	39.2	7.9	37.8	70.5	84.0	42.2	93.8	59.9	61.9	27.7	10.6	56.7	52.5	50.1	50.9	52.1
100M	LAION	68.9	90.5	68.6	23.6	60.6	68.3	7.8	41.2	74.7	87.1	47.7	94.4	45.6	53.4	23.6	10.4	54.5	51.9	53.3	52.8	53.9
	<i>RealSyn</i>	73.5	89.5	68.8	20.1	65.0	48.5	10.2	46.1	76.7	87.6	48.8	94.4	69.0	65.5	24.6	12.1	60.5	52.4	54.1	56.2	56.2

### 3.2 Retrieval and Generation Framework

After extracting high-quality images and sentences from documents, we propose an efficient and scalable framework to retrieve multiple semantically relevant texts for each image and leverage large language models to integrate retrieved realistic text with fine-grained visual information and generate synthetic text. As shown in Figure 3, the architecture of our framework primarily consists of three components: Text Semantic Clustering, Hierarchical Retrieval, and Image Semantic Augmented Generation.

**Text Semantic Clustering.** To efficiently retrieve multiple semantically relevant texts for each image, we initially encode all sentences using the EVA02-CLIP E/14-plus [68] model. Inspired by Unicom [1], we utilize the standard  $K$ -Means algorithm [34] offline cluster all sentences into a specified number of clusters. To minimize intra-cluster and inter-cluster conflicts, we initially establish the optimal number of cluster centroids through small-scale experiments. Subsequently, we divide the 0.84 billion texts into two million clusters, utilizing efficient feature quantization techniques [35].

**Hierarchical Retrieval.** Given the prohibitive computational cost of direct semantic text retrieval across 0.84B sentences (requiring over 10,000 GPU-hours on 8×A100), we propose a hierarchical retrieval framework to enhance efficiency. Given an image, we perform inter-cluster retrieval to identify the most relevant cluster center for the image. Subsequently, we conduct intra-cluster retrieval within the identified cluster to obtain multiple real-world sentences semantically matched to the image. This approach achieves scalable retrieval of 198M images and 0.84B sentences within 40 GPU-hours on an 8×A100.

**Image Semantic Augmented Generation.** Although the retrieved realistic texts achieve satisfactory performance, they exhibit limitations in capturing fine-grained visual semantics. To address this

issue, we introduce the Image Semantic Augmented Generation module. This module initially employs the OFA [75] model to generate a concise caption for each image. We then integrate the open-set image tagging model RAM++ [33], which extracts object detection tags. Considering that RAM++ supports only 4,000 tags, we expand this set to 8,000 by incorporating an additional 4,000 tags derived from real-world sentences. Following CapsFusion [83], we utilize ChatGPT4 Turbo to merge the retrieved realistic texts with concise captions and image tags to construct a 100K instruction dataset (the prompt we used is presented in the supplementary material). Subsequently, we conduct instruction tuning of the LLaMA3-8B model [18] using the LLaMA Factory [86] and deploy the vLLM [40] for large-scale inference. Ultimately, we convert data from 118M multimodal interleaved documents into 198M image-text pairs, where each image is associated with multiple retrieved realistic texts and synthetic texts.

### 3.3 Semantic Balance Sampling

To further improve the quality and diversity of our dataset, we implement semantic balancing sampling across the 198M image-text pairs. Specifically, we use EVA02-CLIP E/14-plus [68] to encode and calculate the cosine similarity between images and synthetic texts. To reduce the impact of OCR-related or mismatched pairs during pre-training, we filter out 29.7M pairs with cosine similarities scores either above 0.61 or below 0.51, as determined through human verification. Inspired by MetaCLIP [32], we introduce an easy but efficient cluster-based semantic balance sampling strategy. We cluster the image embeddings from the remaining 168.3M pairs into 1M centers. To enhance the semantic diversity of our dataset, we randomly select 20, 35, and 180 samples from clusters exceeding these thresholds, while retaining all samples from smaller clusters.

**Table 3: Zero-shot image-text retrieval performance on Flickr30k and MSCOCO. Pre-training CLIP-B/32 on *RealSyn* dataset achieves a significant improvement on all metrics.**

Data Scale	Dataset	Text Retrieval						Image Retrieval					
		Flickr30k			MSCOCO			Flickr30k			MSCOCO		
		R@1	R@5	R@10	R@1	R@5	R@10	R@1	R@5	R@10	R@1	R@5	R@10
15M	YFCC	37.1	64.8	75.9	21.3	45.1	57.0	23.5	47.3	58.3	13.2	32.0	43.1
	LAION	49.1	76.8	84.5	28.4	53.0	64.9	33.3	60.5	70.9	17.4	38.3	49.7
	<i>RealSyn</i>	72.9	91.1	95.1	43.8	69.5	79.6	49.5	76.3	84.6	25.8	50.6	62.5
30M	LAION	59.6	83.5	89.8	35.9	62.4	73.2	42.4	70.1	79.4	22.1	45.5	57.6
	<i>RealSyn</i>	76.0	93.3	96.9	48.2	74.6	83.0	54.0	80.0	87.6	29.5	55.2	66.9
100M	LAION	67.5	87.9	93.0	43.3	68.0	78.1	50.4	77.2	85.5	27.1	52.1	63.8
	<i>RealSyn</i>	81.6	96.1	97.3	52.3	76.7	85.0	58.8	84.1	90.5	32.5	58.9	70.2

**Table 4: Zero-shot robustness comparison on different IN-1K val set variants. Pre-training CLIP-B/32 on *RealSyn* demonstrates superior robustness across all datasets.**

Data Scale	Dataset	IN-V2	IN-A	IN-R	ObjectNet	IN-Sketch	Average
15M	YFCC	27.3	12.3	20.8	25.3	6.3	18.4
	LAION	30.7	6.0	46.5	28.7	24.3	27.2
	<i>RealSyn</i>	37.1	12.5	47.7	35.0	25.4	31.5
30M	LAION	37.5	8.9	54.4	35.5	31.8	33.6
	<i>RealSyn</i>	42.9	16.1	56.6	41.5	31.9	37.8
100M	LAION	44.6	12.2	62.5	42.2	37.9	39.9
	<i>RealSyn</i>	47.6	19.7	62.5	45.8	37.9	42.7

This approach culminates in the construction of the *RealSyn*15M, *RealSyn*30M, and *RealSyn*100M datasets.

## 4 Experiments and Results

### 4.1 Implementation Details

We initially collect 118M interleaved image-text documents from the OBELICS [43] as our primary data source. We use  $OFA_{base}$  [75] and  $RAM++_{large}$  [33] to generate brief captions and semantic tags. To validate the dataset performance, we pre-train standard CLIP supervised by the text randomly selected from the three retrieved realistic texts and one synthetic text, inspired by the LaCLIP [19]. During pre-training, we adopt AdamW [53] as the optimizer, with a learning rate of  $1e-3$  and a weight decay of 0.2. The parameters  $\beta_1$  and  $\beta_2$  are set to 0.9 and 0.98, respectively. The input image size is  $224 \times 224$ , and the input text sequence length is 77. The temperature parameter  $\tau$  is initialized to 0.07. We train 32 epochs with 4096 batch sizes on  $8 \times A100$  (80G) GPUs. Please refer to the supplementary material for more details.

To validate the effectiveness of the *RealSyn* dataset, we compare *RealSyn* with the previous datasets across various models and data scales. We compare *RealSyn*15M with the YFCC15M filtered by DeCLIP [47]. Following ALIP [79], we also compare with LAION15M, LAION30M, and LAION100M (subset randomly selected from LAION400M).

### 4.2 Main Results

**Linear Probe.** In Table 1, we report the linear probe performance of the ViT-B/32 model across 20 downstream datasets. When pre-trained at the 15M scale, *RealSyn*15M exceeds YFCC15M on 16 of 20

datasets, achieving an average performance increase of 6.9%. Additionally, *RealSyn*15M outperforms LAION15M on 18 of 20 datasets, with an average improvement of 1.6%. With dataset scaling to 30M and 100M, *RealSyn* achieves average performance improvements of 1.3% and 1.4% over LAION, respectively. These findings underscore the superior CLIP training efficiency of the *RealSyn* dataset compared to the widely-used YFCC and LAION datasets across multiple scales.

**Zero-shot Transfer.** We evaluate the zero-shot transfer performance of the ViT-B/32 model across 20 classification benchmarks using the same prompt templates as SLIP [57]. As indicated in Table 2, *RealSyn*15M surpasses YFCC15M on 18 of 20 datasets, achieving an average performance improvement of 14.3%. In comparison to LAION15M, *RealSyn*15M excels on 18 of 20 datasets with an average improvement of 5.2%. Upon expanding the dataset sizes to 30M and 100M, *RealSyn* achieves average performance improvements of 3.5% and 2.3% compared to LAION, highlighting its efficiency and scalability.

It is important to note that *RealSyn* demonstrates a significant decrease in performance on certain datasets, such as Cars and Flowers. This reduction is primarily attributed to the unique data distribution of *RealSyn*, characterized by a scarcity of data for specific concepts, which hampers the model’s ability to effectively learn these concepts. For example, as shown in Figure 4, samples related to cars and flowers represent only 0.9% and 0.4% of the dataset, respectively.

**Zero-shot Image-Text Retrieval.** In Table 3, we present the zero-shot image-text retrieval performance of the ViT-B/32 model pre-trained on different scales of datasets. *RealSyn* achieves superior results across all evaluation metrics. Specifically, *RealSyn*15M improves Recall@1 by 35.8%&26% on Flickr30K [82] and by 22.5%&12.6% on MSCOCO [50]. *RealSyn*30M improves Recall@1 by 16.4%&11.6% on Flickr30K [82] and by 12.3%&7.4% on MSCOCO [50]. *RealSyn*100M improves Recall@1 by 14.6%&8.4% on Flickr30K [82] and by 9%&5.4% on MSCOCO [50]. This significant enhancement in cross-modal retrieval performance indicates that the *RealSyn* dataset effectively improves contrastive vision-language representation learning by incorporating both realistic and synthetic texts, resulting in robust representations and enhanced cross-modal alignment.

**Zero-shot Robustness.** To further validate the robustness of the *RealSyn* dataset, we present the zero-shot robustness [62] performance across various IN-1K [17] val set variants in Table 4. The

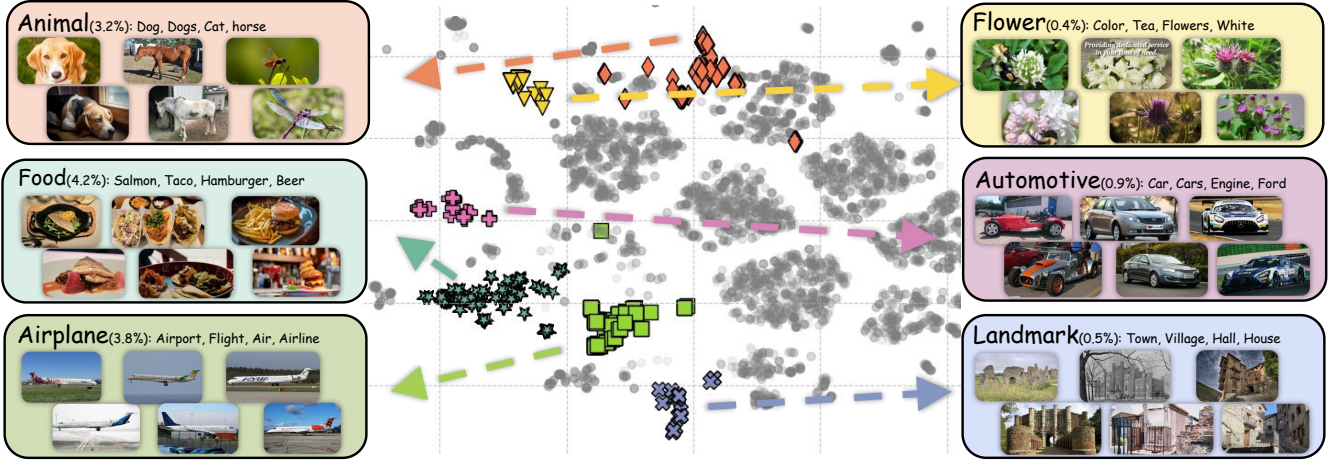


Figure 4: A T-SNE [72] projection of LDA [6] topic cluster from a randomly selected 1M samples from *RealSyn*. *RealSyn* encompasses a broad range of everyday topics, e.g., animal, food, airplane, etc. We also display representative central images for each identified topic.

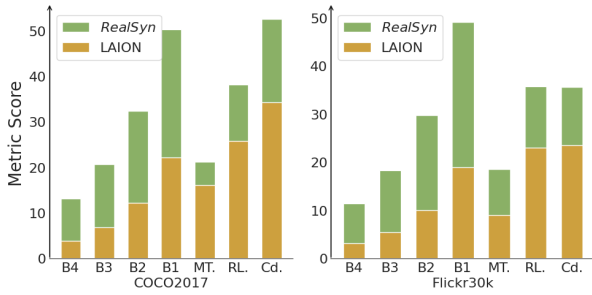
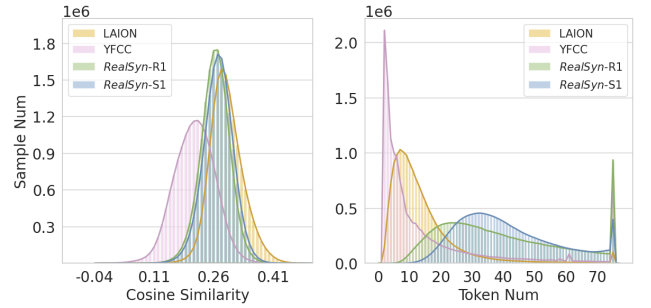


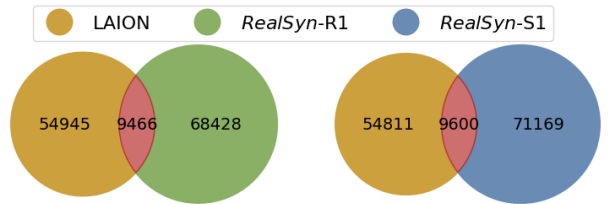
Figure 5: Image captioning comparisons on COCO2017 and Flickr30k. B4, MT, RL, and Cd. represent the metric of BLEU [59], METEOR [3], ROUGE-L [3], and Cider [73].

results indicate that *RealSyn* significantly enhances the robustness of vision-language pre-training models. Specifically, *RealSyn*15M shows a performance increase of 13.1% and 4.3% compared to YFCC15M and LAION15M, respectively. When scaled to 30M and 100M, *RealSyn* achieves additional improvements of 4.2% and 2.8% over LAION. This substantial enhancement in performance is primarily attributable to the utilization of retrieved realistic texts, which surpass the constraints of generative models, and the superior conceptual diversity relative to YFCC and LAION, thus significantly boosting model robustness.

**Image Captioning via MLLM.** In Figure 5, we present the image captioning performance of the LLaVA-1.5 [52] trained using different datasets (LAION v.s. *RealSyn*). Initially, we first map visual features into the textual domain using the initial 558k dataset from LLaVA-1.5. We then develop an image captioning dataset from both LAION and *RealSyn* for instruction tuning. Specifically, we select 1M samples randomly from each dataset and train over two epochs. As depicted in Figure 5, *RealSyn* significantly outperforms LAION in all evaluation metrics on both the COCO2017 [50] and Flickr30k [82] benchmarks. This notable performance enhancement confirms the higher quality and better image-text alignment of the *RealSyn* dataset.



(a) Richness assessment comparison



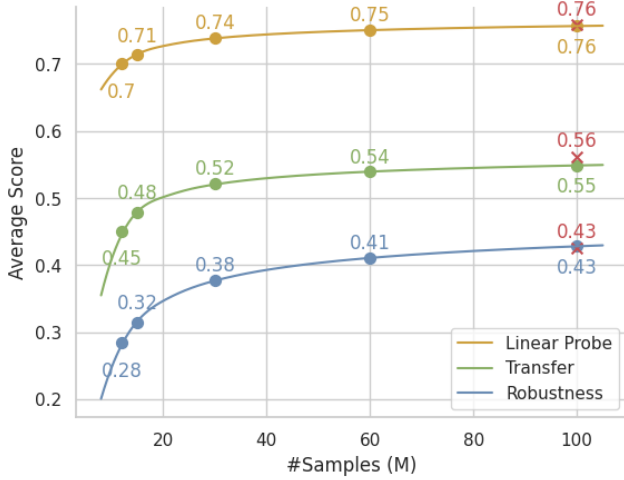
(b) Diversity assessment comparison

Figure 6: The richness assessment and diversity assessment on different datasets. *RealSyn*-R1: the most relevant retrieved realistic text. *RealSyn*-S1: the semantic augmented synthetic text based on *RealSyn*-R1.

## 5 Analysis

### 5.1 Statistics Analysis

**Topic-based Assessment.** Following MMC4 [89], we ran LDA [6] on random sampling 1M image-realistic text pairs with 30 topics. Figure 4 presents the proportions and examples for six topics: animal, food, airplane, flower, automotive, and landmark. Notably, the dataset contains minimal samples related to “flower” and “automotive” topics, representing merely 0.4% and 0.9% of the total, respectively. This paucity of examples hinders the model’s ability



**Figure 7: Data Scaling Analysis.** We pretrain ViT-B/32 on *RealSyn* in different data scales.  $\times$  represents the results predicted using our data scaling law.

to sufficiently learn these concepts, thereby compromising its performance in the linear probe and zero-shot transfer evaluations on the Flowers and Cars datasets.

**Richness Assessment.** Figure 6a presents image-text similarity and text token distribution of 15M samples from YFCC15, LAION, *RealSyn*-R1 (the most relevant retrieved realistic text), and *RealSyn*-S1 (the semantic augmented synthetic text based on *RealSyn*-R1). Compared to datasets sourced from the Internet, *RealSyn* demonstrates robust similarity metrics even after the removal of OCR data. This effectively explains the significant performance enhancement observed in the CLIP model trained on *RealSyn* for image-text retrieval tasks. Moreover, both the retrieved realistic texts and synthetic texts contain a larger quantity of words, which can provide a richer textual context that enhances vision-language representation learning.

**Diversity Assessment.** The *RealSyn* is constructed based on real-world interleaved image-text documents, which encompasses a wide array of diverse information. Following previous work [41], we randomly select 0.2M samples to calculate the number of unique entities in the caption to assess the data diversity of different datasets. As depicted in Figure 6b, both the retrieved realistic texts and image semantic augmented synthetic texts exhibit a higher number of distinct entities. Such diversity enriches the dataset, facilitating the model’s acquisition of comprehensive knowledge and enhancing both performance and robustness.

**Data Scaling Analysis.** We present the data scaling law [36] derived from our *RealSyn* dataset, justifying its scalability over samples. Specifically, we conduct a series of visual-language pre-trainings with proposed datasets ranging from 12M to 60M, and fit each performance metric to the inverse of logarithmic functions with respect to the number of millions of training samples  $x$ . Based on the fitting results from these preliminary experiments, we extrapolate each performance scaling law to 100M samples, and validate their predicted scaling trends with our *RealSyn*100M dataset as shown in Figure 7. Notably, as indicated by the coefficients shown in Eq. 3, these performance laws also likely suggest

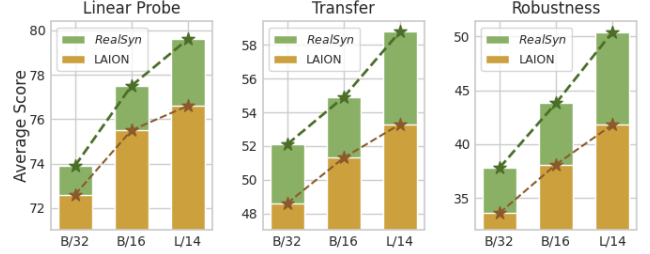


**Figure 8: Model scaling capability.** We compare the models pre-trained on LAION30M and *RealSyn*30M.

**Table 5: Comparison of semantic balance sampling and random sampling on the 15M dataset.**

Model	Dataset	Linear probe Avg	Transfer Avg	Robustness Avg
CLIP-B/32	YFCC	64.5	33.6	18.4
	LAION	69.8	42.7	27.2
	<i>RealSyn</i> -Random	70.7	46.8	30.5
	<i>RealSyn</i> -Balance	71.4	47.9	31.5

an upper bound of model capability that a ViT-B/32 could possibly reach through our proposed visual-language pre-training paradigm with multimodal interleaved documents:

$$\begin{aligned}
 \text{Linear Probe: } \mathcal{L}(x) &\approx \frac{-0.21}{\log(x - 4.23)} + 0.80 \\
 \text{Transfer: } \mathcal{L}(x) &\approx \frac{-0.30}{\log(x - 5.68)} + 0.62 \\
 \text{Robustness: } \mathcal{L}(x) &\approx \frac{-0.60}{\log(x - 3.17)} + 0.56
 \end{aligned} \tag{3}$$

**Model Scaling Analysis.** In Section 4.2, *RealSyn* exhibits superior performance across various data scales. To further explore the model scaling capability, we present the downstream task performance of three models in Figure 8. Notably, compared to LAION, *RealSyn* demonstrates steeper slopes in performance curves across linear probe, zero-shot transfer, and robustness, indicative of its superior model scaling capabilities.

**Extension to Pure Image.** To further extend our transformation paradigm for pure images, we conduct experiments on ImageNet [17]. Initially, we retrieve semantically relevant realistic texts for each ImageNet image from our sentence database and generate image semantic augmented synthetic texts. Then, we pre-train ResNet50 [28] supervised by the text randomly selected from the retrieved realistic texts and synthetic texts. Comparative analysis with SimCLR [11] under identical conditions shows a linear probe average performance enhancement of 2.1% across 12 datasets using our constructed data. Detailed experimental results are provided in the supplementary material.

## 5.2 Ablation Study

**Ablation on Semantic Balance Sampling.** To demonstrate the efficacy of our proposed semantic balance sampling method, we contrast it with random sampling. As shown in Table 5, semantic balance sampling achieves performance improvements of 0.7%,



**Table 6: Ablation study examining the quantity and combinations of retrieved realistic texts and corresponding image semantic augmented synthetic texts within a 15M-scale dataset.  $T_r^k$ : the  $k$ -th retrieved semantic relevant realistic text.  $T_s^k$ : the image semantic augmented synthetic text for  $T_r^k$ .**

$T_r^1$	$T_r^2$	$T_r^3$	$T_r^4$	$T_r^5$	Linear probe Avg	$T_s^1$	$T_s^2$	$T_s^3$	$T_s^4$	$T_s^5$	Linear probe Avg	$T_r^1$	$T_r^2$	$T_r^3$	$T_s^1$	Linear probe Avg	Transfer Avg	Robustness Avg
✓					70.3	✓					70.2	✓				70.3	42.4	25.7
✓	✓				71.0	✓	✓				70.0	✓	✓			71.2	46.8	30.7
✓	✓	✓			71.2	✓	✓	✓			69.9	✓	✓	✓		70.2	39.7	24.0
✓	✓	✓	✓		70.9	✓	✓	✓	✓		69.4	✓			✓	71.4	47.9	31.5
✓	✓	✓	✓	✓	70.6	✓	✓	✓	✓	✓	69.1	✓	✓	✓	✓			

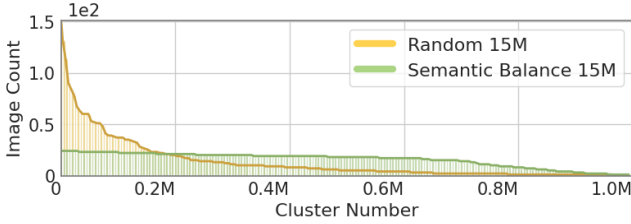


**Figure 9: Clustering distribution of 15M data obtained from random sampling and semantic balance sampling.**

1.1%, and 1.0% in linear probe accuracy, zero-shot transfer, and robustness, respectively. Besides, we visualize the data distribution of 15M samples clustered into 1M centers using different sampling strategies. As shown in Figure 9 reveals that semantic balance sampling results in a smoother distribution, thereby enhancing the learning of long-tail concepts.

**Ablation on Realistic Texts and Synthetic Texts.** We conduct ablation studies to assess the impact of varying quantities of realistic and synthetic texts on the performance of the CLIP-B/32 model. As shown in Table 6, incrementally increasing the amount of realistic text from one to three enhances model performance, attributed to improved text augmentation that integrates extensive real-world knowledge. However, further increasing this quantity from three to five slightly diminishes performance due to information saturation and the introduction of noise. Conversely, augmenting the number of synthetic texts from one to five incrementally degrades performance, reflecting increased noise introduction. Notably, training with only realistic texts significantly boosts performance, achieving a 71.2% accuracy compared to 69.8% with the LAION15M dataset, underscoring the vital role of real-world knowledge in advancing vision-language representation learning.

**Ablation on the Combination of the Realistic Texts and Synthetic Texts.** Table 6 presents the results of ablation experiments on text augmentation using different text types. Introducing image semantic augmented synthetic text, which supplements fine-grained visual semantic information, leads to performance enhancements of 0.2%, 1.1%, and 0.8% in linear probe accuracy, zero-shot transfer, and zero-shot robustness, respectively, compared to using only retrieved realistic texts.

**Case Study.** In Figure 10, we present the visualization of retrieved realistic text and synthetic text obtained from an interleaved image-text document using our proposed transformation paradigm. Both realistic and synthetic texts contain extensive descriptive information consistent with the image semantics, such as “lyell glacier”,

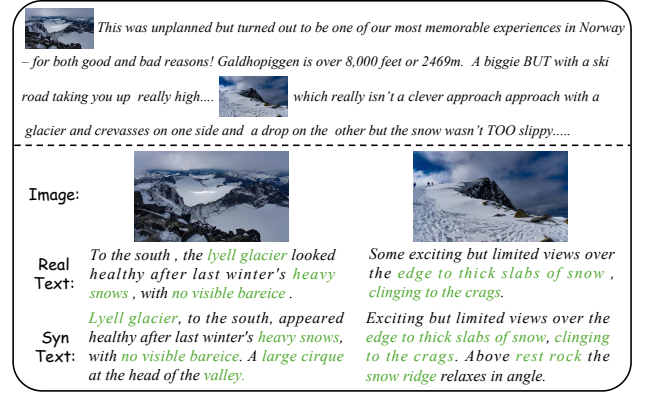


**Figure 10: Visualization of the raw interleaved document, the retrieved realistic text, and synthetic text. Image semantic-related information is highlighted in green.**

“crag”, and “valley”. We provide more visualizations in the supplementary material.

## 6 Conclusion

This paper explores two open-ended questions: 1) How to utilize multimodal interleaved documents for CLIP training. 2) How to effectively leverage both realistic and synthetic texts to enhance CLIP performance. To this end, we first establish a Real-World Data Extraction pipeline to extract high-quality images and texts. Then we design a hierarchical retrieval method to efficiently associate each image with multiple semantically relevant texts. To further enhance fine-grained visual information, we propose an image semantic augmented generation module for synthetic text production. Furthermore, we employ a semantic balance sampling strategy to improve dataset diversity, enabling better learning of long-tail concepts. Based on these innovations, we present *RealSyn*, a dataset driven by both real and synthetic texts with three sizes: 15M, 30M, and 100M. We compare our dataset with other widely used datasets of equivalent scale for CLIP training. Models pre-trained on *RealSyn* consistently achieve state-of-the-art performance across various downstream tasks. Furthermore, extensive experiments confirm that *RealSyn* significantly enhances contrastive vision-language representation learning and demonstrates robust scalability. We hope our work provides insights into vision-language representation learning.





## References

- [1] Xiang An, Jiankang Deng, Kaicheng Yang, Jiawei Li, Ziyong Feng, Jia Guo, Jing Yang, and Tongliang Liu. 2023. Unicom: Universal and Compact Representation Learning for Image Retrieval. In *ICLR*.
- [2] Tadas Baltrušaitis, Chaitanya Ahuja, and Louis-Philippe Morency. 2018. Multimodal machine learning: A survey and taxonomy. *TPAMI* (2018).
- [3] Satantjeet Banerjee and Alon Lavie. 2005. METEOR: An automatic metric for MT evaluation with improved correlation with human judgments. In *ACL*.
- [4] Thomas Berg, Jiongxin Liu, Seung Woo Lee, Michelle L. Alexander, David W. Jacobs, and Peter N. Belhumeur. 2014. Birdsnap: Large-scale fine-grained visual categorization of birds. In *CVPR*.
- [5] Steven Bird and Edward Loper. 2004. NLTK: The Natural Language Toolkit. In *ACL*.
- [6] David M Blei, Andrew Y Ng, and Michael I Jordan. 2003. Latent dirichlet allocation. *JMLR* (2003).
- [7] Lukas Bossard, Matthieu Guillaumin, and Luc Van Gool. 2014. Food-101—mining discriminative components with random forests. In *ECCV*.
- [8] Minwoo Byeon, Beomhee Park, Haechon Kim, Sungjun Lee, Woonhyuk Baek, and Saehoon Kim. 2022. COYO-700M: Image-Text Pair Dataset. <https://github.com/kakaobrain/coyo-dataset>.
- [9] Soravit Changpinyo, Piyush Sharma, Nan Ding, and Radu Soricut. 2021. Conceptual 12m: Pushing web-scale image-text pre-training to recognize long-tail visual concepts. In *CVPR*.
- [10] Lin Chen, Jisong Li, Xiaoyi Dong, Pan Zhang, Conghui He, Jiaqi Wang, Feng Zhao, and Dahua Lin. 2024. ShareGPT4V: Improving Large Multi-Modal Models with Better Captions. In *ECCV*.
- [11] Ting Chen, Simon Kornblith, Mohammad Norouzi, and Geoffrey Hinton. 2020. A simple framework for contrastive learning of visual representations. In *ICML*.
- [12] Xinlei Chen, Hao Fang, Tsung-Yi Lin, Ramakrishna Vedantam, Saurabh Gupta, Piotr Dollár, and C Lawrence Zitnick. 2015. Microsoft coco captions: Data collection and evaluation server. *arXiv:1504.00325* (2015).
- [13] Gong Cheng, Junwei Han, and Xiaoqiang Lu. 2017. Remote sensing image scene classification: Benchmark and state of the art. *Proc. IEEE* (2017).
- [14] Mircea Cimpoi, Subhransu Maji, Iasonas Kokkinos, Sammy Mohamed, and Andrea Vedaldi. 2014. Describing textures in the wild. In *CVPR*.
- [15] Christopher Clark and Matt Gardner. 2017. Simple and effective multi-paragraph reading comprehension. In *ACL*.
- [16] Adam Coates, Andrew Ng, and Honglak Lee. 2011. An analysis of single-layer networks in unsupervised feature learning. In *AISTATS*.
- [17] Jia Deng, Wei Dong, Richard Socher, Li-Jia Li, Kai Li, and Li Fei-Fei. 2009. ImageNet: A large-scale hierarchical image database. In *CVPR*.
- [18] Abhimanyu Dubey, Abhinav Jauhri, Abhinav Pandey, Abhishek Kadian, Ahmad Al-Dahle, Aiesha Letman, Akhil Mathur, Alan Schelten, Amy Yang, Angela Fan, et al. 2024. The llama 3 herd of models. *arXiv:2407.21783* (2024).
- [19] Lijie Fan, Dilip Krishnan, Phillip Isola, Dina Katabi, and Yonglong Tian. 2024. Improving clip training with language rewrites. In *NeurIPS*.
- [20] Li Fei-Fei, Rob Fergus, and Pietro Perona. 2004. Learning generative visual models from few training examples: An incremental bayesian approach tested on 101 object categories. In *CVPR*.
- [21] Samir Yitzhak Gadre, Gabriel Ilharco, Alex Fang, Jonathan Hayase, Georgios Smyrnis, Thao Nguyen, Ryan Marten, Mitchell Wortsman, Dhruva Ghosh, Jieyu Zhang, et al. 2024. Datacomp: In search of the next generation of multimodal datasets. In *NeurIPS*.
- [22] Andreas Geiger, Philip Lenz, and Raquel Urtasun. 2012. Are we ready for autonomous driving? the kitti vision benchmark suite. In *CVPR*.
- [23] Yash Goyal, Tejas Khot, Douglas Summers-Stay, Dhruv Batra, and Devi Parikh. 2017. Making the v in vqa matter: Elevating the role of image understanding in visual question answering. In *CVPR*.
- [24] Tiancheng Gu, Kaicheng Yang, Xiang An, Ziyong Feng, Dongnan Liu, Weidong Cai, and Jiankang Deng. 2024. Rwkv-clip: A robust vision-language representation learner. In *EMNLP*.
- [25] Qiushan Guo, Shalini De Mello, Hongxu Yin, Wonmin Byeon, Ka Chun Cheung, Yizhou Yu, Ping Luo, and Sifei Liu. 2024. Regiongpt: Towards region understanding vision language model. In *CVPR*.
- [26] Ruohao Guo, Liao Qu, Dantong Niu, Yanyu Qi, Wenzhen Yue, Ji Shi, Bowei Xing, and Xianghua Ying. 2024. Open-Vocabulary Audio-Visual Semantic Segmentation. In *ACMMM*. 7533–7541.
- [27] Wenzhong Guo, Jianwen Wang, and Shiping Wang. 2019. Deep multimodal representation learning: A survey. *IEEE Access* (2019).
- [28] Kaiming He, Xiangyu Zhang, Shaoqing Ren, and Jian Sun. 2016. Deep residual learning for image recognition. In *CVPR*.
- [29] Wenbin He, Suphanut Jamonnak, Liang Gou, and Liu Ren. 2023. Clip-s4: Language-guided self-supervised semantic segmentation. In *Proceedings of the IEEE/CVF conference on computer vision and pattern recognition*. 11207–11216.
- [30] Patrick Helber, Benjamin Bischke, Andreas Dengel, and Damian Borth. 2019. Eurosat: A novel dataset and deep learning benchmark for land use and land cover classification. *IEEE Journal of Selected Topics in Applied Earth Observations and Remote Sensing* (2019).
- [31] Xiaoxing Hu, Kaicheng Yang, Jun Wang, Haoran Xu, Ziyong Feng, and Yupei Wang. 2025. Decoupled Global-Local Alignment for Improving Compositional Understanding. *arXiv preprint arXiv:2504.16801* (2025).
- [32] Xiaoqing Ellen Tan Hu Xu, Saining Xie. 2023. Demystifying CLIP Data. *arXiv:2309.16671* (2023).
- [33] Xinyu Huang, Yi-Jie Huang, Youcai Zhang, Weiwei Tian, Rui Feng, Yuejie Zhang, Yanchun Xie, Yaqian Li, and Lei Zhang. 2023. Inject semantic concepts into image tagging for open-set recognition. *arXiv:2310.15200* (2023).
- [34] Abiodun M. Ikotun, Absalom E. Ezugwu, Laith Abualigah, Belal Abuhaija, and Jia Heming. 2023. K-means clustering algorithms: A comprehensive review, variants analysis, and advances in the era of big data. *Inf. Sci.* (2023).
- [35] Jeff Johnson, Matthijs Douze, and Hervé Jégou. 2019. Billion-scale similarity search with GPUs. *IEEE Transactions on Big Data* 7, 3 (2019), 535–547.
- [36] Jared Kaplan, Sam McCandlish, Tom Henighan, Tom B Brown, Benjamin Chess, Rewon Child, Scott Gray, Alec Radford, Jeffrey Wu, and Dario Amodei. 2020. Scaling laws for neural language models. *arXiv preprint arXiv:2001.08361* (2020).
- [37] Douwe Kiela, Hamed Firooz, Aravind Mohan, Vedanuj Goswami, Amanpreet Singh, Pratik Ringshia, and Davide Testuggine. 2020. The hateful memes challenge: Detecting hate speech in multimodal memes. In *NeurIPS*.
- [38] Jonathan Krause, Michael Stark, Jia Deng, and Li Fei-Fei. 2013. 3d object representations for fine-grained categorization. In *ICCV*.
- [39] Alex Krizhevsky, Geoffrey Hinton, et al. 2009. Learning multiple layers of features from tiny images. *Technical Report* (2009).
- [40] Woosuk Kwon, Zhuohan Li, Siyuan Zhuang, Ying Sheng, Lianmin Zheng, Cody Hao Yu, Joseph Gonzalez, Hao Zhang, and Ion Stoica. 2023. Efficient memory management for large language model serving with pagedattention. In *SOSP*.
- [41] Zhengfeng Lai, Vasileios Saveris, Chen Chen, Hong-You Chen, Haotian Zhang, Bowen Zhang, Juan Lao Tebar, Wenzhe Hu, Zhe Gan, Peter Gräsch, et al. 2025. Revisit Large-Scale Image-Caption Data in Pre-training Multimodal Foundation Models. In *ICLR*.
- [42] Zhengfeng Lai, Haotian Zhang, Bowen Zhang, Wentao Wu, Haoping Bai, Aleksei Timofeev, Xianzhi Du, Zhe Gan, Jiulong Shan, Chen-Nee Chuah, Yinfei Yang, and Meng Cao. 2024. VeCLIP: Improving CLIP Training via Visual-enriched Captions. In *ECCV*.
- [43] Hugo Laurençon, Lucile Saulnier, Léo Tronchon, Stas Bekman, Amanpreet Singh, Anton Lozhkov, Thomas Wang, Siddharth Karamcheti, Alexander Rush, Douwe Kiela, et al. 2024. Obelics: An open web-scale filtered dataset of interleaved image-text documents. In *NeurIPS*.
- [44] Junnan Li, Dongxu Li, Silvio Savarese, and Steven Hoi. 2023. Blip-2: Bootstrapping language-image pre-training with frozen image encoders and large language models. In *International conference on machine learning*. PMLR, 19730–19742.
- [45] Qingyun Li, Zhe Chen, Weiyun Wang, Wenhai Wang, Shenglong Ye, Zhenjiang Jin, et al. 2025. OmniCorpus: A Unified Multimodal Corpus of 10 Billion-Level Images Interleaved with Text. In *ICLR*.
- [46] Xiaotong Li, Fan Zhang, Haiwen Diao, Yueze Wang, Xinlong Wang, and Ling-Yu Duan. 2024. Densefusion-1m: Merging vision experts for comprehensive multimodal perception. In *NeurIPS*.
- [47] Yangguang Li, Feng Liang, Lichen Zhao, Yufeng Cui, Wanli Ouyang, Jing Shao, Fengwei Yu, and Junjie Yan. 2022. Supervision Exists Everywhere: A Data Efficient Contrastive Language-Image Pre-training Paradigm. In *ICLR*.
- [48] Zichao Li, Cihang Xie, and Ekin Dogus Cubuk. 2024. Scaling (down) clip: A comprehensive analysis of data, architecture, and training strategies. *arXiv preprint arXiv:2404.08197* (2024).
- [49] Jiayi Lin and Shaogang Gong. 2023. Gridclip: One-stage object detection by grid-level clip representation learning. *arXiv preprint arXiv:2303.09252* (2023).
- [50] Tsung-Yi Lin, Michael Maire, Serge Belongie, James Hays, Pietro Perona, Deva Ramanan, Piotr Dollár, and C Lawrence Zitnick. 2014. Microsoft coco: Common objects in context. In *ECCV*.
- [51] Yuqi Lin, Minghao Chen, Wenxiao Wang, Boxi Wu, Ke Li, Binbin Lin, Haifeng Liu, and Xiaofei He. 2023. Clip is also an efficient segmenter: A text-driven approach for weakly supervised semantic segmentation. In *CVPR*. 15305–15314.
- [52] Haotian Liu, Chunyuan Li, Yuheng Li, and Yong Jae Lee. 2024. Improved baselines with visual instruction tuning. In *CVPR*.
- [53] I Loshchilov. 2019. Decoupled Weight Decay Regularization. In *ICLR*.
- [54] Subhransu Maji, Esa Rahtu, Juho Kannala, Matthew Blaschko, and Andrea Vedaldi. 2013. Fine-grained visual classification of aircraft. *arXiv:1306.5151* (2013).
- [55] Ségolène Martin, Yunshi Huang, Fereshth Shakeri, Jean-Christophe Pesquet, and Ismail Ben Ayed. 2024. Transductive Zero-Shot and Few-Shot CLIP. In *CVPR*.
- [56] Ron Mokady, Amir Hertz, and Amit H Bermano. 2021. Clipcap: Clip prefix for image captioning. *arXiv preprint arXiv:2111.09734* (2021).
- [57] Norman Mu, Alexander Kirillov, David Wagner, and Saining Xie. 2022. Slip: Self-supervision meets language-image pre-training. In *ECCV*.
- [58] Maria-Elena Nilsback and Andrew Zisserman. 2008. Automated flower classification over a large number of classes. In *Sixth Indian Conference on Computer Vision, Graphics & Image Processing*.
- [59] Kishore Papineni, Salim Roukos, Todd Ward, and Wei-Jing Zhu. 2002. Bleu: a method for automatic evaluation of machine translation. In *ACL*.

- [60] Omkar M Parkhi, Andrea Vedaldi, Andrew Zisserman, and CV Jawahar. 2012. Cats and dogs. In *ICCV*.
- [61] Filip Radenovic, Abhimanyu Dubey, Abhishek Kadian, Todor Mihaylov, Simon Vandenhende, Yash Patel, Yi Wen, Vignesh Ramanathan, and Dhruv Mahajan. 2023. Filtering, distillation, and hard negatives for vision-language pre-training. In *CVPR*.
- [62] Alec Radford, Jong Wook Kim, Chris Hallacy, Aditya Ramesh, Gabriel Goh, Sandhini Agarwal, Girish Sastry, Amanda Askell, Pamela Mishkin, Jack Clark, et al. 2021. Learning transferable visual models from natural language supervision. In *ICML*.
- [63] Alec Radford, Jeffrey Wu, Rewon Child, David Luan, Dario Amodei, Ilya Sutskever, et al. 2019. Language models are unsupervised multitask learners. *OpenAI blog* (2019).
- [64] Christoph Schuhmann, Romain Beaumont, Richard Vencu, Cade Gordon, Ross Wightman, Mehdi Cherti, Theo Coombes, Aarush Katta, Clayton Mullis, Mitchell Wortsman, Patrick Schramowski, Srivatsa Kundurthy, Katherine Crowson, Ludwig Schmidt, Robert Kaczmarczyk, and Jenia Jitsev. 2022. LAION-5B: An open large-scale dataset for training next generation image-text models. In *NeurIPS*.
- [65] Christoph Schuhmann, Richard Vencu, Romain Beaumont, Robert Kaczmarczyk, Clayton Mullis, Aarush Katta, Theo Coombes, Jenia Jitsev, and Aran Komatsuzaki. 2021. Laion-400m: Open dataset of clip-filtered 400 million image-text pairs. In *NeurIPS Workshop*.
- [66] Shuai Shao, Yu Bai, Yan Wang, Baodi Liu, and Yicong Zhou. 2024. DeLL: Direct-and-Inverse CLIP for Open-World Few-Shot Learning. In *CVPR*.
- [67] Khurram Soomro, Amir Roshan Zamir, and Mubarak Shah. 2012. UCF101: A dataset of 101 human actions classes from videos in the wild. *arXiv:1212.0402* (2012).
- [68] Quan Sun, Yuxin Fang, Ledell Wu, Xinlong Wang, and Yue Cao. 2023. Eva-clip: Improved training techniques for clip at scale. *arXiv:2303.15389* (2023).
- [69] Yuwei Tang, Zhenyi Lin, Qilong Wang, Pengfei Zhu, and Qinghua Hu. 2024. AMU-Tuning: Effective Logit Bias for CLIP-based Few-shot Learning. In *CVPR*.
- [70] Robert Endre Tarjan. 1975. Efficiency of a good but not linear set union algorithm. *JACM* (1975).
- [71] Bart Thomee, David A Shamma, Gerald Friedland, Benjamin Elizalde, Karl Ni, Douglas Poland, Damian Borth, and Li-Jia Li. 2016. YFCC100M: The new data in multimedia research. *Commun. ACM* (2016).
- [72] Laurens Van der Maaten and Geoffrey Hinton. 2008. Visualizing data using t-SNE. *JMLR* (2008).
- [73] Ramakrishna Vedantam, C Lawrence Zitnick, and Devi Parikh. 2015. Cider: Consensus-based image description evaluation. In *CVPR*.
- [74] Jingyun Wang and Guoliang Kang. 2024. Learn to Rectify the Bias of CLIP for Unsupervised Semantic Segmentation. In *CVPR*.
- [75] Peng Wang, An Yang, Rui Men, Junyang Lin, Shuai Bai, Zhikang Li, Jianxin Ma, Chang Zhou, Jingren Zhou, and Hongxia Yang. 2022. Ofa: Unifying architectures, tasks, and modalities through a simple sequence-to-sequence learning framework. In *ICML*.
- [76] Xiao Wang, Ibrahim Alabdulmohsin, Daniel Salz, Zhe Li, Keran Rong, and Xiaohua Zhai. 2025. Scaling Pre-training to One Hundred Billion Data for Vision Language Models. *arXiv preprint arXiv:2502.07617* (2025).
- [77] Xiaoshi Wu, Feng Zhu, Rui Zhao, and Hongsheng Li. 2023. Cora: Adapting clip for open-vocabulary detection with region prompting and anchor pre-matching. In *CVPR*. 7031–7040.
- [78] Jianxiong Xiao, James Hays, Krista A Ehinger, Aude Oliva, and Antonio Torralba. 2010. Sun database: Large-scale scene recognition from abbey to zoo. In *ICCV*.
- [79] Kaicheng Yang, Jiankang Deng, Xiang An, Jiawei Li, Ziyong Feng, Jia Guo, Jing Yang, and Tongliang Liu. 2023. Alip: Adaptive language-image pre-training with synthetic caption. In *ICCV*.
- [80] Kaicheng Yang, Tiancheng Gu, Xiang An, Haiqiang Jiang, Xiangzi Dai, Ziyong Feng, Weidong Cai, and Jiankang Deng. 2025. CLIP-CID: Efficient CLIP Distillation via Cluster-Instance Discrimination. In *AAAI*.
- [81] Ruilin Yao, Shengwu Xiong, Yichen Zhao, and Yi Rong. 2024. Visual Grounding with Multi-modal Conditional Adaptation. In *ACMMM*. 3877–3886.
- [82] Peter Young, Alice Lai, Micah Hodosh, and Julia Hockenmaier. 2014. From image descriptions to visual denotations: New similarity metrics for semantic inference over event descriptions. *TACL* (2014).
- [83] Qiying Yu, Quan Sun, Xiaosong Zhang, Yufeng Cui, Fan Zhang, Yue Cao, Xinlong Wang, and Jingjing Liu. 2024. Capsfusion: Rethinking image-text data at scale. In *CVPR*.
- [84] Changmeng Zheng, Dayong Liang, Wengyu Zhang, Xiao-Yong Wei, Tat-Seng Chua, and Qing Li. 2024. A Picture Is Worth a Graph: A Blueprint Debate Paradigm for Multimodal Reasoning. In *ACMMM*. 419–428.
- [85] Kecheng Zheng, Yifei Zhang, Wei Wu, Fan Lu, Shuailei Ma, Xin Jin, Wei Chen, and Yujun Shen. 2024. DreamLIP: Language-Image Pre-training with Long Captions. In *ECCV*.
- [86] Yaowei Zheng, Richong Zhang, Junhao Zhang, Yanhan Ye, Zheyang Luo, Zhangchi Feng, and Yongqiang Ma. 2024. LlamaFactory: Unified Efficient Fine-Tuning of 100+ Language Models. In *ACL*.
- [87] Ziqin Zhou, Yinjie Lei, Bowen Zhang, Lingqiao Liu, and Yifan Liu. 2023. Zegclip: Towards adapting clip for zero-shot semantic segmentation. In *CVPR*. 11175–11185.
- [88] Jiaqi Zhu, Shaofeng Cai, Fang Deng, Beng Chin Ooi, and Junran Wu. 2024. Do LLMs Understand Visual Anomalies? Uncovering LLM's Capabilities in Zero-shot Anomaly Detection. In *ACMMM*. 48–57.
- [89] Wanrong Zhu, Jack Hessel, Anas Awadalla, Samir Yitzhak Gadre, Jesse Dodge, Alex Fang, Youngjae Yu, Ludwig Schmidt, William Yang Wang, and Yejin Choi. 2024. Multimodal c4: An open, billion-scale corpus of images interleaved with text. In *NeurIPS*.



This supplementary material introduces the experiment settings and the instruction prompt we used in Section A. Then, we introduce the downstream datasets, detailed model scaling results, comparison with the rewrite datasets, and analyze the combination *RealSyn* with LAION and detailed results on pure image in Section B. We further analyze our proposed *RealSyn* dataset by comparison with current datasets and visualize examples in Section C. Finally, we discuss the limitations of this paper in Section D.

## A Detail Experiment Settings

### A.1 Experiment Settings

In Table 7, we present the detailed settings used in training CLIP.

**Table 7: Hyperparameters used for CLIP pre-training.**

Hyperparameter	Value
Initial temperature	0.07
Weight decay	0.2
Batch size	4096
Learning rate	0.001
Learning rate scheduler	OneCycleLR
Pct start	0.1
Training epochs	32
GPU	8×A100
Adam $\beta_1$	0.9
Adam $\beta_2$	0.98
Adam $\epsilon$	$10^{-6}$

### A.2 Detail Instruction Prompt

The prompt we used for ChatGPT to construct the 100K instruction dataset is present in the following:

*"Please merge the information from the given raw text and the synthetic caption with the help of the highly relevant detection tags. The raw caption offers detailed real-world information, yet it suffers from flaws in sentence structure and grammar. The synthetic caption exhibits impeccable sentence structure but often lacks in-depth real-world details and may contain false information. The highly relevant detection tags are provided to enrich the semantic information of the raw caption, while some are redundant and noisy. You are a great information integration and summary expert, you are also good at enriching semantic information. Ensure a well-structured sentence while retaining the detailed real-world information provided in the raw caption. Avoid simply concatenating the sentences and avoid adding external information to describe. Correct and simplify sentences finally. Raw caption:<raw caption>, synthetic caption:<synthetic caption>, and highly relevant detection tags:<detection tags>".*

## B Detail External Results

### B.1 Downstream Datasets

To demonstrate the performance of CLIP trained on *RealSyn*, we compared the linear probe results of CLIP trained on *RealSyn*,

YFCC [71], and LAION [65] across 20 datasets. These datasets include Food101 [7], CIFAR10 [39], CIFAR100 [39], Birdsnap [4], SUN397 [78], Stanford Cars [38], FGVC Aircraft [54], DTD [14], Pets [60], Caltech101 [20], Flowers102 [58], SLT10 [16], EuroSAT [30], RESISC45 [13], KITTI [22], Country211 [62], UCF101 [67], Hateful Memes [37], SST2 [62], and ImageNet [17]. Details on each dataset and the corresponding evaluation metrics are provided in Table 8.

**Table 8: List of linear probe datasets with the data distribution and evaluation metrics.**

Dataset	Classes	Train size	Test size	Evaluation metric
Food101	102	75,750	25,250	accuracy
CIFAR10	10	50,000	10,000	accuracy
CIFAR100	100	50,000	10,000	accuracy
Birdsnap	500	42,138	2,149	accuracy
SUN397	397	19,850	19,850	accuracy
Cars	196	8,144	8,041	accuracy
Aircraft	100	6,667	3,333	mean per class
DTD	47	3,760	1,880	accuracy
Pets	37	3,680	3,669	mean per class
Caltech101	101	3,000	5,677	mean per class
Flowers	102	2,040	6,149	mean per class
STL10	10	5,000	8,000	accuracy
EuroSAT	10	10,000	5,000	accuracy
RESISC45	45	3,150	25,200	accuracy
KITTI	4	6770	711	accuracy
Country211	211	42,200	21,100	accuracy
UCF101	101	9,537	1,794	accuracy
Memes	2	8,500	500	ROC AUC
SST2	2	7,792	1,821	accuracy
ImageNet	1000	1,281,167	50,000	accuracy

### B.2 Detailed Model Scaling Results

**Linear Probe.** In Table 9, we present the detailed linear probe results of different scale CLIP models trained on the 30M dataset. The ViT-L/14 trained on *RealSyn*30M achieves an average performance improvement of 3.0% across 20 datasets compared to the model trained on the LAION30M.

**Zero-shot Transfer.** As shown in Table 10, ViT-L/14 trained on our proposed *RealSyn*30M outperforms LAION30M on 18 of 20 downstream datasets and achieves an average improvement of 5.5%.

**Zero-shot Robustness.** We present the detailed zero-shot robustness performance in Table 11, compared with LAION30M, the model trained on *RealSyn*30M boosts average robustness performance by 8.6% on ViT-L/14.

### B.3 Comparison with the Rewrite Dataset.

Due to LaCLIP [19] and Capsfusion [83] do not provide the model weights trained on the same scale dataset as ours, We compared the same scale model ViT-B/16 pre-trained on the *RealSyn* with DreamLIP [85].

As shown in Table 12, ViT-B/16 pre-trained on *RealSyn*15M can achieve 1.3% and 8.3% average improvement compared to DreamLIP proposed 15M Rewriting datasets based on YFCC15M [71]. Furthermore, compared with DreamLIP's proposed 30M, which combines



**Table 9: Linear probe on 20 downstream datasets. Pre-training different scale CLIP models on *RealSyn30M* and *LAION30M*, achieves 1.3%-3.0% average performance improvement.**

Model	Dataset	Food101	CIFAR10	CIFAR100	Birdsnap	SUN397	Cars	Aircraft	DTD	Pets	Caltech	Flowers	STL10	EuroSAT	RESISC45	KITTI	Country	UCF101	Memes	SST2	ImageNet	Average
ViT-B/32	LAION	76.1	94.5	80.0	47.4	70.3	82.3	45.9	74.7	80.3	89.8	89.5	95.6	95.5	84.5	72.6	15.2	76.6	56.2	60.0	64.3	72.6
	<i>RealSyn</i>	81.2	95.4	81.8	48.4	74.5	73.4	45.2	74.2	84.1	91.3	90.6	97.2	96.5	89.2	74.5	19.0	82.6	55.0	56.2	68.5	73.9
ViT-B/16	LAION	82.1	95.1	81.4	57.5	73.4	87.3	47.1	76.1	84.4	91.5	92.7	96.8	95.6	86.8	70.8	17.6	80.3	59.5	65.6	68.8	75.5
	<i>RealSyn</i>	87.5	95.8	82.5	59.4	77.5	81.0	48.7	77.9	88.9	92.5	94.2	98.3	96.9	91.5	70.8	22.1	85.1	60.6	64.7	73.9	77.5
ViT-L/14	LAION	84.7	96.4	83.5	59.2	75.5	88.5	46.6	77.8	85.0	92.6	94.3	97.9	95.9	88.0	71.7	18.7	81.1	58.6	64.6	71.2	76.6
	<i>RealSyn</i>	90.3	97.5	86.2	64.3	79.7	83.6	51.4	79.6	90.0	94.5	94.8	98.9	96.6	92.7	73.8	25.0	86.4	63.8	66.1	76.7	79.6

**Table 10: Zero-shot transfer on 20 downstream datasets. Pre-training different scale CLIP models on *RealSyn30M* and *LAION30M*, achieves 3.5%-5.5% average performance improvement.**

Model	Dataset	Food101	CIFAR10	CIFAR100	Birdsnap	SUN397	Cars	Aircraft	DTD	Pets	Caltech	Flowers	STL10	EuroSAT	RESISC45	KITTI	Country	UCF101	Memes	SST2	ImageNet	Average
ViT-B/32	LAION	58.9	85.9	63.1	17.4	54.8	61.0	4.3	36.4	65.5	82.0	41.3	91.3	40.3	43.7	24.3	7.2	47.4	51.5	50.1	44.9	48.6
	<i>RealSyn</i>	67.5	89.0	65.2	15.0	60.6	39.2	7.9	37.8	70.5	84.0	42.2	93.8	59.9	61.9	27.7	10.6	56.7	52.5	50.1	50.9	52.1
ViT-B/16	LAION	67.6	89.1	63.5	20.8	55.7	66.9	5.4	39.0	70.2	84.9	42.9	94.3	31.1	45.4	34.0	8.7	52.2	54.5	50.6	49.4	51.3
	<i>RealSyn</i>	75.8	89.6	64.7	18.9	64.3	48.2	7.9	41.2	76.0	87.5	45.2	95.1	56.8	64.3	27.1	13.1	59.1	54.5	54.0	55.9	54.9
ViT-L/14	LAION	70.8	88.8	69.5	22.8	61.6	69.7	4.9	40.8	68.0	87.3	42.2	95.3	41.5	53.7	25.9	10.4	54.7	54.1	51.8	51.5	53.3
	<i>RealSyn</i>	80.7	94.1	73.1	20.9	66.4	53.6	10.1	48.1	72.8	89.4	49.8	96.2	68.5	70.1	32.2	15.3	63.9	54.1	56.9	59.5	58.8

**Table 11: Zero-shot robustness comparison. Pre-training different scale CLIP models on *RealSyn30M* and *LAION30M*, achieves 4.2%-8.6% average performance improvement.**

Model	Dataset	IN-V2	IN-A	IN-R	ObjectNet	IN-Sketch	Average
ViT-B/32	LAION	37.5	8.9	54.4	35.5	31.8	33.6
	<i>RealSyn</i>	42.9	16.1	56.5	41.5	31.9	37.8
ViT-B/16	LAION	42.4	12.8	60.3	40.2	34.8	38.1
	<i>RealSyn</i>	48.0	24.1	63.1	46.7	36.8	43.8
ViT-L/14	LAION	45.1	17.1	64.9	43.1	39.0	41.8
	<i>RealSyn</i>	52.8	34.7	71.6	50.4	42.4	50.4

**Table 12: Comparison with DreamLIP’s rewriting dataset.**

Model	Data Scale	Dataset	Linear probe Avg	Transfer Avg
ViT-B/16	15M	DreamLIP	73.7	43.3
		<i>RealSyn</i>	74.9	51.6
	30M	DreamLIP	77.2	53.1
		<i>RealSyn</i>	77.5	54.9

YFCC15M, CC12M [9] and CC3M [9] dataset, ViT-B/16 training on *RealSyn30M* can also outperform it in the linear probe and zero transfer. This significant improvement indicates that realistic knowledge is important for the CLIP model.

#### B.4 Combine *RealSyn* with LAION

As shown in Table 13, integrating *RealSyn15M* with LAION15M yields average improvements of 0.6% in linear probe, 0.2% in zero-shot transfer across 20 datasets, and a robustness increase of 0.6% compared to LAION30M. Comparing *RealSyn30M* with LAION30M,

the former shows significant performance gains, with average improvements of 1.3% in linear probe, 3.5% in zero-shot transfer, and a robustness enhancement of 4.2%. The experimental results demonstrate that *RealSyn* when combined with existing datasets, achieves significant performance improvements, while also validating the robustness and extensibility of *RealSyn*.

**Table 13: Data Scaling Comparison. Merged 30M: LAION 15M + *RealSyn15M*.**

Model	Dataset	Linear probe Avg	Transfer Avg	Robustness Avg
ViT-B/16	LAION15M	69.8	42.7	27.2
	<i>RealSyn15M</i>	71.4	47.9	31.5
	LAION30M	72.6	48.6	33.6
	Merged30M	73.2	48.8	34.2
	<i>RealSyn30M</i>	73.9	52.1	37.8

#### B.5 Detailed Results on Pure Image

To further extend our method for pure images, we conduct experiments on ImageNet [17]. For each image, we retrieve three semantically relevant real-world sentences from our pre-constructed sentence database and generate a single semantically augmented synthetic caption based on the top retrieved text. Following SimCLR [11], we utilize 4096 batch size and pre-train ResNet50 [28] for 90 epochs supervised by the text randomly selected from the three retrieved realistic texts and one synthetic text.

As shown in Table 14, compared with SimCLR [11] under the same conditions, the model trained on our constructed image-text pairs shows an average performance improvement of 2.1% across 12 downstream datasets. The results demonstrate that our method can

**Table 14: Linear probe on 12 downstream datasets. Pre-training CLIP (ResNet50) on image-text pairs achieves 2.1% performance improvement.**

Model	Method	Food101	CIFAR10	CIFAR100	Birdsnap	SUN397	Cars	Aircraft	VOC2007	DTD	Pets	Calech101	Flowers	Average
ResNet50	SimCLR	68.4	90.6	71.6	37.4	58.8	50.3	50.3	80.5	74.5	83.6	90.3	91.2	70.6
	Real&Syn Texts	72.5	89.1	69.0	57.1	63.6	51.4	48.1	85.5	69.7	90.5	88.1	88.8	72.7

**Table 15: Current Dataset Comparison. Comparison with large-scale image-text pre-training datasets.**

Dataset	#Images	#Avg Tokens / Image	#Avg Texts / Image	Text Type	Source Type
CC12M	12 000 000	–	1	Realistic	Website
YFCC15M	15 000 000	16	1	Realistic	Website
CapsFusion	120 000 000	–	1	Synthetic	Image-Text Pair
LAION400M	400 000 000	27	1	Realistic	Website
RealSyn15M	15 239 498	40	4	Realistic & Synthetic	Interleaved Image-Text
RealSyn30M	30 328 852	38	4	Realistic & Synthetic	Interleaved Image-Text
RealSyn100M	100 862 786	36	4	Realistic & Synthetic	Interleaved Image-Text

effectively transform pure images into high-quality image-text pairs through retrieval and generation for vision-language pre-training.

## C Further Analysis of RealSyn

### C.1 Compare with Existing Datasets

In Table 15, we compare our proposed *RealSyn* dataset with existing widely used large-scale image-text pre-training datasets. Compared to previous datasets, our proposed *RealSyn* dataset provides four textual descriptions for each image, with an average token length of 36-40, significantly higher than LAION400M and YFCC15M. Furthermore, unlike previous datasets, the *RealSyn* dataset is sourced from real-world interleaved image-text documents and includes both realistic and synthetic texts, thereby expanding the scope for future research exploration.

### C.2 Visualization of Examples

In Figure 11 and Figure 12, we visualize additional image-text pairs randomly selected from our proposed *RealSyn* dataset.  $T_r^k$  is the

$k$ -th retrieved semantically relevant real-world sentence and  $T_s^k$  is the semantic augmentic caption for  $T_r^k$ . We also highlighted the image semantic-related information in green and marked the image size below the image.

## D Limitations

To provide more fine-grained visual information, this study employs vision expert models in conjunction with a Large Language Model (LLM) to generate synthetic text. Considering inference costs and efficiency, further exploration of Modified Large Language Models (MLLM) for synthetic text creation is suggested for the community. Additionally, constrained by computational resources, this paper constructs a 100M-scale *RealSyn* dataset exclusively using OBELICS [43]. Notably, the transformation paradigm presented here is directly applicable to other multimodal document datasets, including MMC4 [89] and OmniCorpus [45].

Raw Image:

 $T_r^1$  : $T_r^2$  : $T_r^3$  : $T_s^1$  :

(506, 336)

This was a good *gig* !. grass street was an *exceptional group* to play at my husband's 60th birthday bash .

The headlining *band* was a local *band* he was using on a katrina benefit album & they had invited him to drop by .

We did our first *reunion show* in 2010 [ after coming together in 2009 to celebrate the life of longtime friend and former employee paul ducharme ].

Grass street was an *exceptional group* to play at my husband's 60th birthday bash , and they played instruments like *guitars*, *drums*.



(448, 336)

It is not often the case that *depression* is simply a layer on top of a personality , the metaphorical "*dark cloud* ", but instead it is something deeply ingrained .

Lifting the shroud of *mystery* on *depression* . it 's a topic that has vast implications for human health .

Creators who are yet *struggling* to breakthrough often get into *depression* .

*Depression* is not just a superficial layer on top of a personality , but rather it is deeply ingrained , like a *dark cloud* .



(505, 336)

This large *beach* allows guests to grab and *hammock* or a *lounge chair* and relax .

Enjoy the beach club and all the *equipment* on the *island* !

*Loungers* are arranged on the hotel 's rocky private *beach* opposite .

Guests can relax on the *large beach* with chairs , hammocks , and daybeds under the *palm trees* , enjoying the *ocean view* .



(448, 336)

*Cheers* and enjoy the *beach* !

I hope the *sky* is *blue* at your place . *cheers* from the *beach* at coquette point .

Great *pics* and even in winter a *drink* on a *beach* sounds bliss .

Enjoy the *sunset* while *sipping* a cup of *beer* on the *beach* .



(598, 336)

There are currently around 6 , 5 0 0 *petrol stations* ." this is just the beginning of the *infrastructure* build out ."

Nevertheless , the *infrastructure* needed already exists as a network of filling *stations* .

Additionally , a *tank fuel station* was built in java in 2006 as well .

There are currently around 6 , 5 0 0 *petrol stations* , which is just the beginning of the *infrastructure* build out .



(401, 336)

There are *photos* , such as the 1863 *image* of the construction of the great south *road* .

figure 2 . excavation on the bengal - nagpur *railway* ( 1890 ). figure 2 shows a panoramic *view* of , again , the bengal - nagpur *railway* .

it was during that period that they made this photograph of forest creek which was being turned over by *thousands* of *eager miners* searching for gold .

1863 *image* of the construction of the great south *road* is shown in the *old black and white photo* , with trees along the road .

Figure 11: Visualization of image-text pairs in our proposed RealSyn dataset.  $T_r^k$ : the  $k$ -th retrieved realistic text.  $T_s^k$ : the image semantic augmented synthetic text for  $T_r^k$ . Image semantic-related information is highlighted in green.









Raw Image:	$T_r^1$ :	$T_r^2$ :	$T_r^3$ :	$T_s^1$ :
 (448, 336)	<i>My neighbor claims they still have <b>sticky residue</b> on some of their <b>kitchen surfaces</b> today .</i>	<i>Did you just <b>wipe the counter</b> with a <b>soapy substance</b> to clean it ?</i>	<i>The countertop is sprayed with <b>lysol</b> , which destroys the germs , and they are <b>wiped away clean</b> .</i>	<i>A <b>kitchen counter</b> with a sink and a <b>bottle of cleaning agent</b>, there is foam on the sink.</i>
 (503, 306)	<i>While the sound was intimidating , the sight of the <b>water stream</b> sent shivers down my <b>spine</b> ...</i>	<i>The <b>sound of water</b> flowing from barger 's way is ever present .</i>	<i><b>Flowing water</b> is <b>mesmerizing</b> , <b>blocking out</b> distractions of forest and mind .</i>	<i>Sight of the stream of <b>water with rocks</b> in the forest sent shivers down my <b>spine</b> , <b>despite the</b> intimidating sound .</i>
 (336, 336)	<i>Last week future posted a photo of <b>himself</b> rocking one of the <b>sweater</b> .</i>	<i>At what point are we going to say , you know what , he stole future 's <b>style</b> and we can 't condone this !?</i>	<i>According to his body statistics , future reaches a <b>height of 6 feet 2 inches</b> and weighs about 8 7 kg .</i>	<i>Last week , future posted a photo of <b>himself wearing a white sweater and sunglasses</b> , looking like a rapper .</i>
 (336, 405)	<i>Now there is probably a video game where you can virtually <b>cross stitch</b> your heart 's sayings .</i>	<i>And finally , the background image references the trend of <b>cross - stitching</b> funny quotes .</i>	<i>But it was an impulsive moment of pattern deviation that <b>unlocked the</b> subversive potential of <b>cross - stitch</b> for her .</i>	<i>Now there is probably a video game where you can virtually <b>cross stitch</b> your <b>heart 's sayings</b> , such as " love is not an emotion ."</i>
 (336, 448)	<i>Today , september 4 , is the feast of saint <b>mosheh</b> , better known in most western culture as <b>moses</b> .</i>	<i>To day in the orthodox church we commemorate the lord 's friend and prophet <b>moses</b> , the <b>man of god</b> .</i>	<i>We prayed to st <b>moses</b> so that he may intercede to dispel this pandemic from humanity .</i>	<i>Feast of saint <b>mosheh</b> , also known as <b>moses</b> , is celebrated today , september 4 th , in most western cultures . The man in blue sweater.</i>
 (336, 461)	<i>Photos of <b>birds</b> with their <b>wings spread open</b> , can be a true image of god .</i>	<i>To regain grace he became a <b>bird of flight</b> .</i>	<i>The sight of a <b>bird in flight</b> invoked the feeling of envy in their heart .</i>	<i>Photos of an eagle with their <b>wings spread open</b> , flying in the sky with the <b>sunset</b> in the background , can be a true image of god .</i>

Figure 12: Visualization of image-text pairs in our proposed RealSyn dataset.  $T_r^k$ : the  $k$ -th retrieved realistic text.  $T_s^k$ : the image semantic augmented synthetic text for  $T_r^k$ . Image semantic-related information is highlighted in green.